Solvent and ligand substitution effects on electrocatalytic reduction of CO2 with [Mo(CO)4(x,x'-dimethyl-2,2'-bipyridine)] (x = 4-6) enhanced at a gold cathodic surface

Article

Supplemental Material

Electronic Supporting Information

Experimental

Materials

Tetrahydrofuran (THF, Fisher) was freshly distilled from sodium and benzophenone (purple ketyl radicals) under a dry nitrogen atmosphere. *N*-methy-2-pyrrolidone (NMP, anhydrous, Sigma-Aldrich) was bubbled with dry argon on a frit before use. The supporting electrolyte Bu_4NPF_6 (TBAH, >99.8%, Agro-Organics) was recrystallized twice from hot ethanol and dried under vacuum. All electrochemical measurements and synthetic operations were carried out under atmosphere of dry argon, using standard Schlenk techniques. Where necessary, solutions were saturated with CO_2 (99.99%, BOC) by bubbling on a frit at an atmospheric pressure.

Methods

Cyclic Voltammetry

Cyclic voltammetry (CV) was performed on a PGStat 302N potentiostat (Metrohm Autolab) operated with the NOVA 1.9 software. An air-tight single-compartment three-electrode cell was used in all experiments. A platinum (128 µm) or gold (130 µm) microdisc polished carefully with a 0.25 µm diamond paste (Sommer) served as the working electrode. A coiled platinum wire protected by a glass mantle served as the counter electrode. A coiled silver wire protected by a glass mantle was employed as a pseudo-reference electrode. Ferrocene (Fc) was added for the final potential scans as the internal standard, and all electrode potentials are reported against the Fc/Fc^+ couple. CV samples contained 1 mM analyte and 0.1 M supporting electrolyte.

Infrared and UV-vis Spectroelectrochemistry

Infrared spectroelectrochemistry (SEC) was performed with a Bruker Vertex 70v FT-IR spectrometer equipped with a DTLaGS detector. UV-vis spectroelectrochemistry was performed on a Scinco S-3100 diode-array spectrophotometer, in parallel with the IR monitoring. The course of the controlled-potential spectroelectrochemical experiment was recorded using thin-layer cyclic voltammetry (TL-CV) with an OTTLE cell[1] operated by the EmStat3 or EmStat3+ (PalmSens) potentiostats and the PSTrace 4.2 software. The OTTLE cell was equipped with either a Pt or Au minigrid-working electrode, a platinum minigrid counter electrode, an Ag-wire pseudo-reference electrode and CaF_2 windows. SEC samples contained 3 mM analyte and 0.3 M supporting electrolyte.

Table S1: Electrochemical potentials of $[Mo(CO)_4(x,x'\text{-dmbipy})]$ (x = 4-6) and their reduction products in THF/Bu_4NPF_6, using an Au disc microelectrode.

Redox Step	*E* / V vs Fc/Fc^+		
	x = 4	x = 5	x = 6
$[Mo(CO)_4(dmbipy)] \leftrightarrow [Mo(CO)_4(dmbipy)]^{\bullet-}$ (R1)	-2.15[a]	-2.19[a]	-2.13[a]
$[Mo(CO)_4(dmbipy)]^{\bullet-} \leftrightarrow [Mo(CO)_4(dmbipy)]^{2-}$ (R2)	-2.67[b]	-2.73[b]	-2.69[b]
$[Mo(CO)_3(dmbipy)]^{2-} \leftrightarrow [Mo(CO)_3(dmbipy)]^{\bullet-}$ (O2')	-2.39[c]	-2.36[c]	-2.42[c]

[a] $E_{1/2}$ values. [b] $E_{p,c}$ values. [c] $E_{p,a}$ values. Potentials for $[Mo(CO)_4(bipy)]$ are: R1: -2.05 V ($E_{1/2}$), R2: -2.63 V ($E_{p,c}$) and O2': -2.32 V ($E_{p,a}$).[2]

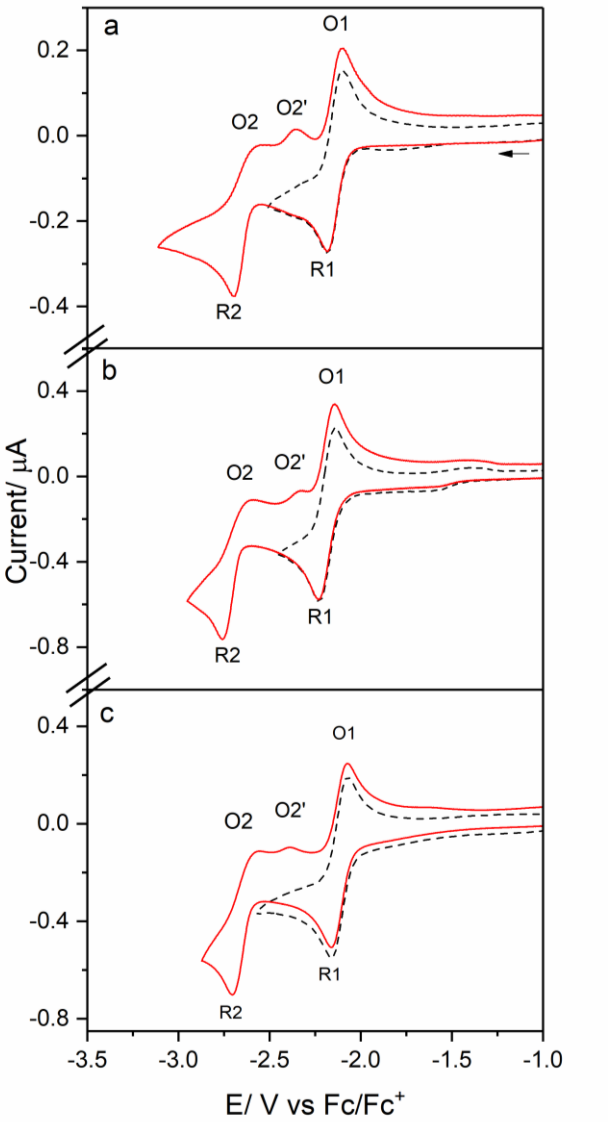

Figure S1: CV of $[Mo(CO)_4(x,x'\text{-dmbipy})]$ in THF/Bu_4NPF_6. (a) x = 4. (b) x = 5. (c) x = 6. Scan rate: 100 mV s^{-1}. Au disc microelectrode. The arrow indicates initial scan direction.

Table S2: Electrode potentials of [Mo(CO)$_4$(x,x'-dmbipy)] (x = 4-6) and their reduction products in NMP/Bu$_4$NPF$_6$, using a Pt disc microelectrode.

Redox Step	*E* / V vs Fc/Fc$^+$		
	x = 4	x = 5	x = 6
[Mo(CO)$_4$(dmbipy)] ↔ [Mo(CO)$_4$(dmbipy)]$^{\bullet-}$	-2.02[a]	-2.06[a]	-1.98[a]
[Mo(CO)$_4$(dmbipy)]$^{\bullet-}$ ↔ [Mo(CO)$_4$(dmbipy)]$^{2-}$	-2.65[b]	-2.73[b]	-2.63[b]
[Mo(CO)$_3$(dmbipy)]$^{2-}$ ↔ [Mo(CO)$_3$(dmbipy)]$^{\bullet-}$	-2.41[c]	-2.37[c]	-[d]

[a] $E_{1/2}$ values. [b] $E_{p,c}$ values. [c] $E_{p,a}$ values. [d]Not observed. Potentials for [Mo(CO)$_4$(bipy)] are: R1: -1.95 V ($E_{1/2}$), R2: -2.71 V ($E_{p,c}$).[2]

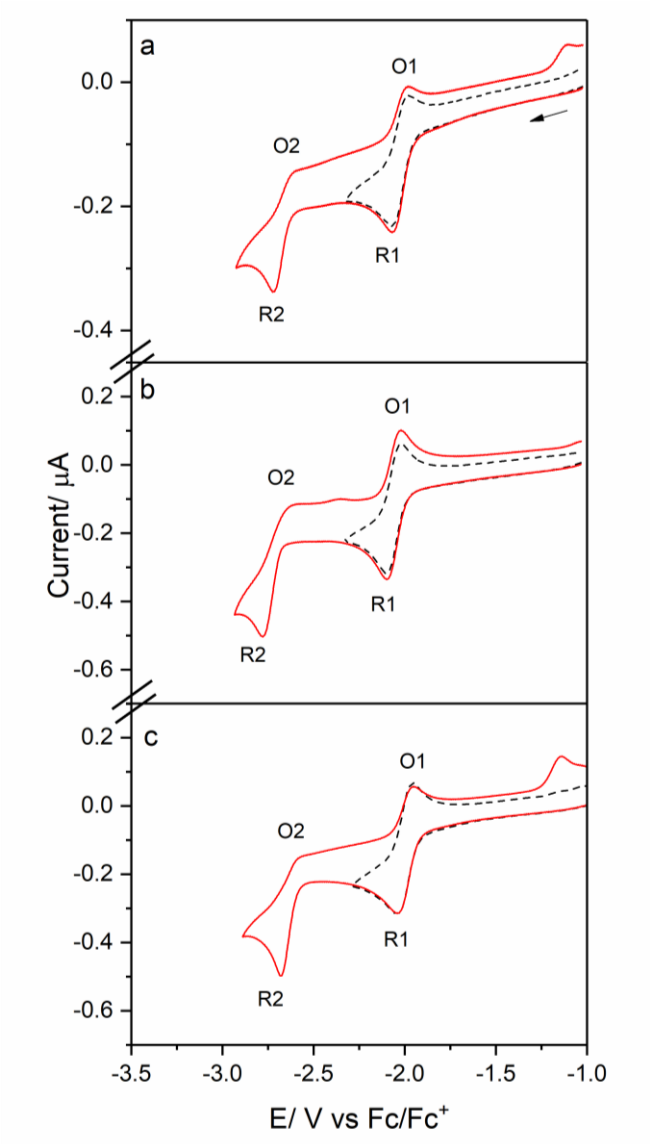

Figure S2: CV of [Mo(CO)$_4$(x,x'-dmbipy)] in NMP/Bu$_4$NPF$_6$. (a) x = 4. (b) x = 5. (c) x = 6. Scan rate: 100 mV s^{-1}. Pt disc microelectrode. The arrow indicates initial scan direction

Table S3: Electrode potentials of [Mo(CO)$_4$(x,x'-dmbipy)] (x = 4-6) and their reduction products in NMP/Bu$_4$NPF$_6$, using an Au disc microelectrode.

Redox Step	*E* / V vs Fc/Fc$^+$		
	x = 4	x = 5	x = 6
[Mo(CO)$_4$(dmbipy)] ↔ [Mo(CO)$_4$(dmbipy)]$^{\bullet-}$	-2.02[a]	-2.06[a]	-1.99[a]
[Mo(CO)$_4$(dmbipy)]$^{\bullet-}$ ↔ [Mo(CO)$_4$(dmbipy)]$^{2-}$	-2.63[b]	-2.69[b]	-2.64[b]
[Mo(CO)$_3$(dmbipy)]$^{2-}$ ↔ [Mo(CO)$_3$(dmbipy)]$^{\bullet-}$	-2.38[c]	-2.38[c]	-[d]

[a] $E_{1/2}$ values. [b] $E_{p,c}$ values. [c] $E_{p,a}$ values. [d]Not observed. Potentials for [Mo(CO)$_4$(bipy)] are: R1: -1.95 V ($E_{1/2}$), R2: -2.71 V ($E_{p,c}$) and O2': -2.22 V ($E_{p,a}$).[2]

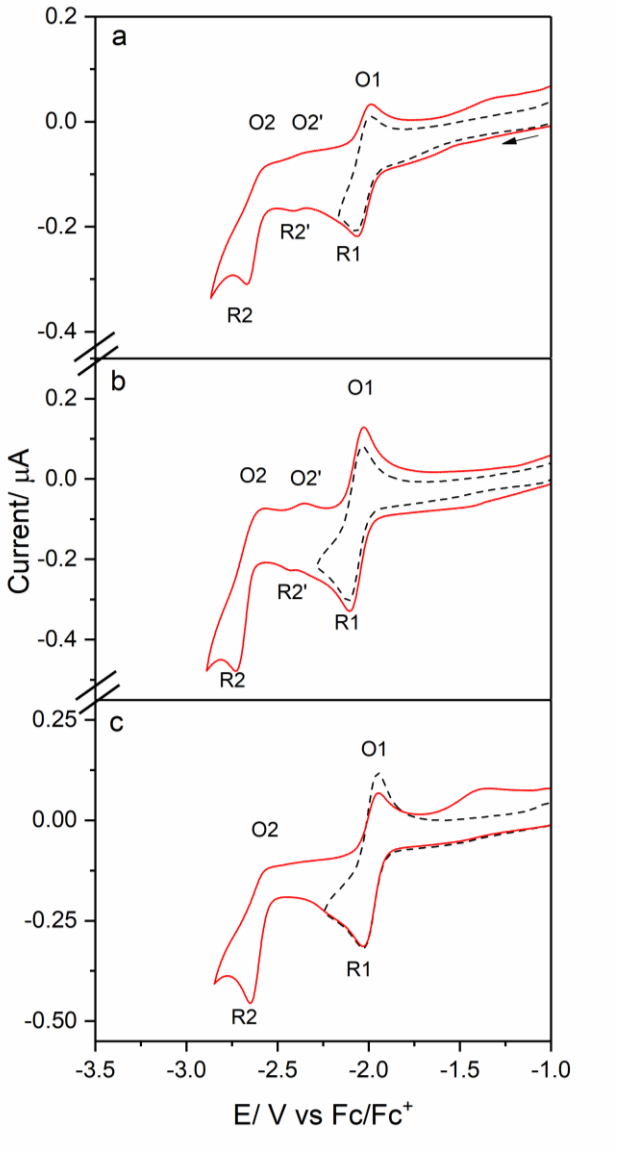

Figure S3: CV of [Mo(CO)$_4$(x,x'-dmbipy)] in NMP/Bu$_4$NPF$_6$. (a) x = 4. (b) x = 5. (c) x = 6. Scan rate: 100 mV s^{-1}. Au disc microelectrode. The arrow indicates initial scan direction.

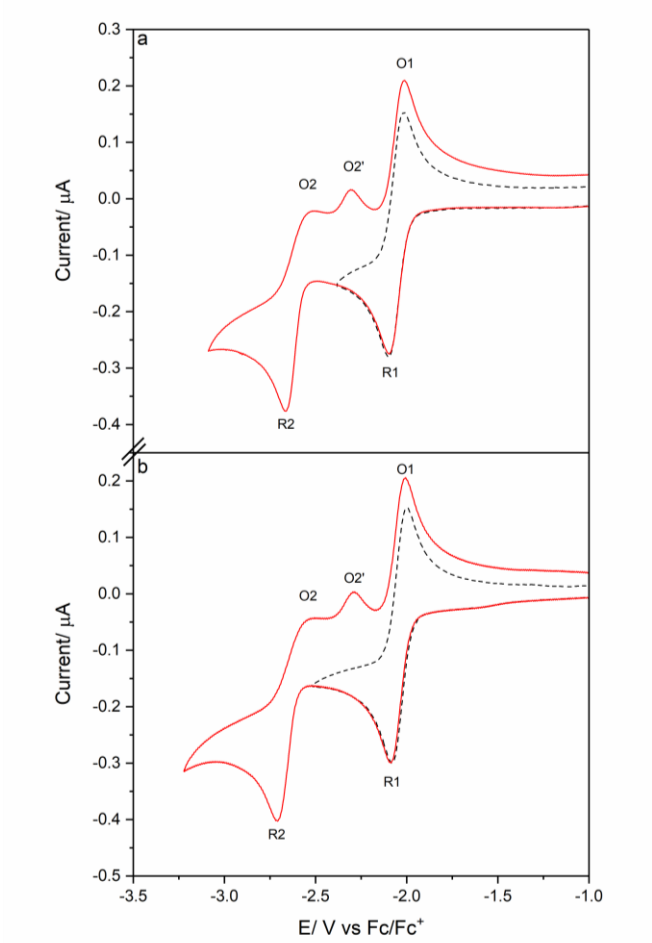

Figure S4: CV of $[Mo(CO)_4(bipy)]$ in THF/Bu_4NPF_6, using (a) an Au disc and, (b) a Pt disc microelectrode. Scan Rate: 100 mV s^{-1}.

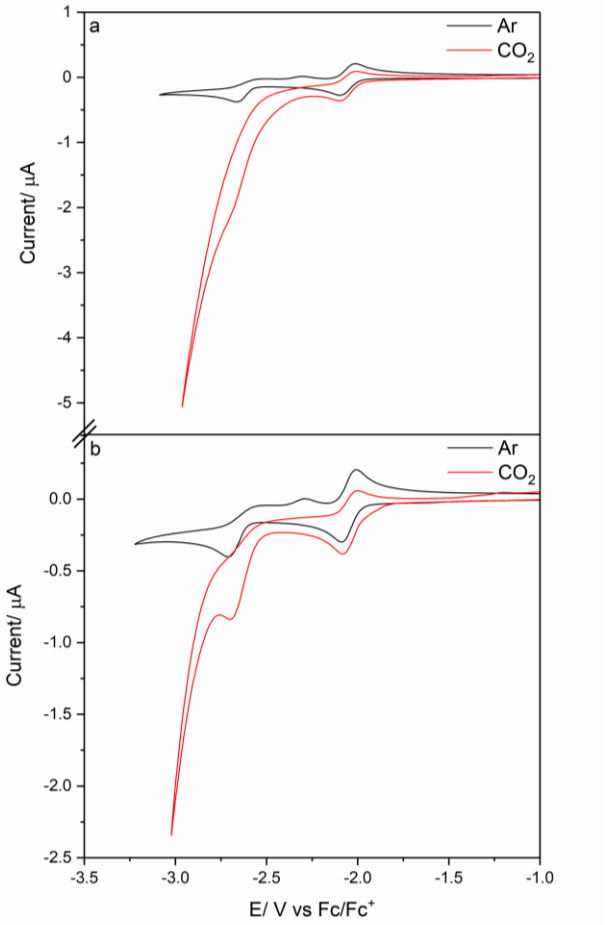

Figure S5: CV of $[Mo(CO)_4(bipy)]$ in CO_2-saturated THF/Bu_4NPF_6, using (a) an Au disc, and (b) using a Pt disc microelectrode. Scan rate: 100 mV s^{-1}.

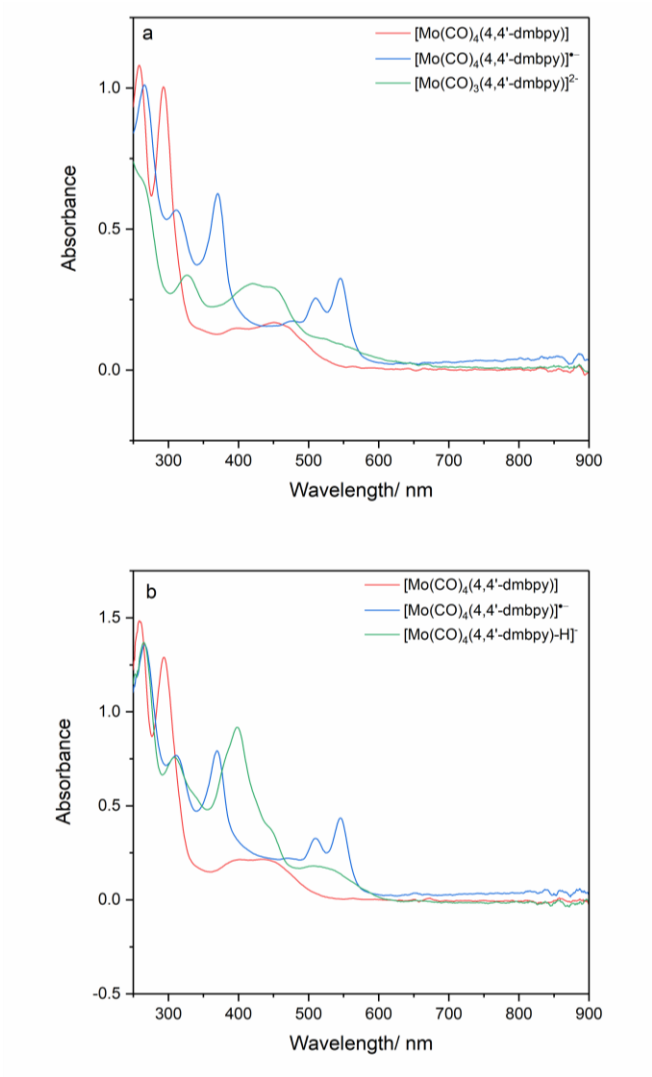

Figure S6. Cathodic UV-vis SEC in (a) THF/Bu_4NPF_6 and (b) NMP/Bu_4NPF_6, showing the conversion of parent [$Mo(CO)_4$(4,4'-dmbipy)] (red) to its radical anion (blue), and finally to dominant 5-coordinate [$Mo(CO)_3$(4,4'-dmbipy)]$^{2-}$ (green, in THF) or [$Mo(CO)_4$(4,4'-dmbipy-H)]$^-$ (green, in NMP).

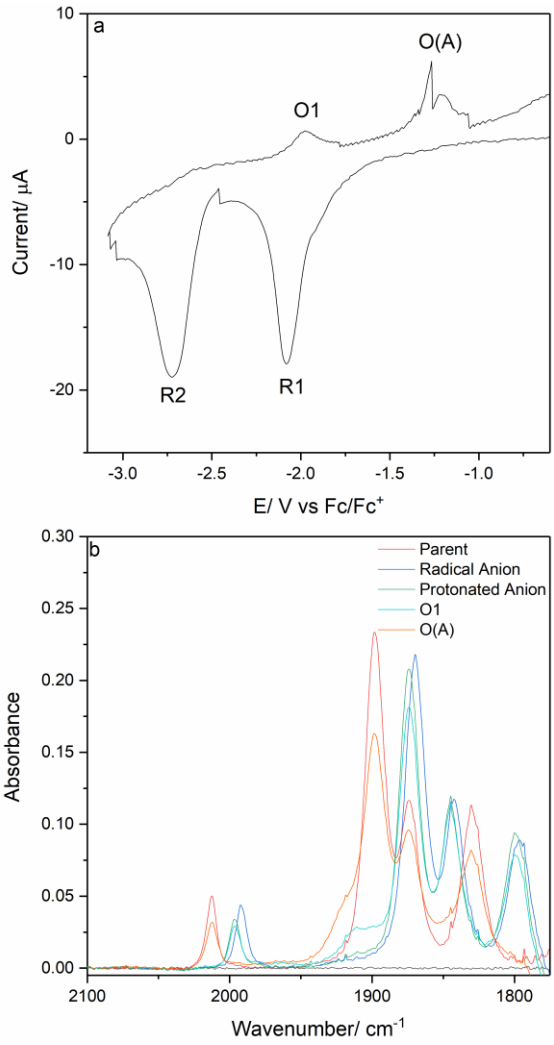

Figure S7. (a)Thin-layer cyclic voltammogram of [$Mo(CO)_4$(4,4'-dmbipy)] in argon-saturated NMP (v = 2 mV s^{-1} recorded at ambient conditions within an OTTLEcell. It shows the stepwise one-electron reduction to [$Mo(CO)_4$(4,4'-dmbipy)]$^{\bullet-}$ at R1, and the latter to [$Mo(CO)_4$(4,4'-dmbipy-H)]$^-$ at R2. The anodic wave O(A) on the reverse scan corresponds to the oxidation of [$Mo(CO)_4$(4,4'-dmbipy-H)]$^-$ that leads to a substantial recovery of parent [$Mo(CO)_4$(4,4'-dmbipy)]. (b) These TL-CV processes were monitored in parallel with IR SEC; CO-stretching wavenumbers of the involved carbonyl complexes are listed in Table 2.

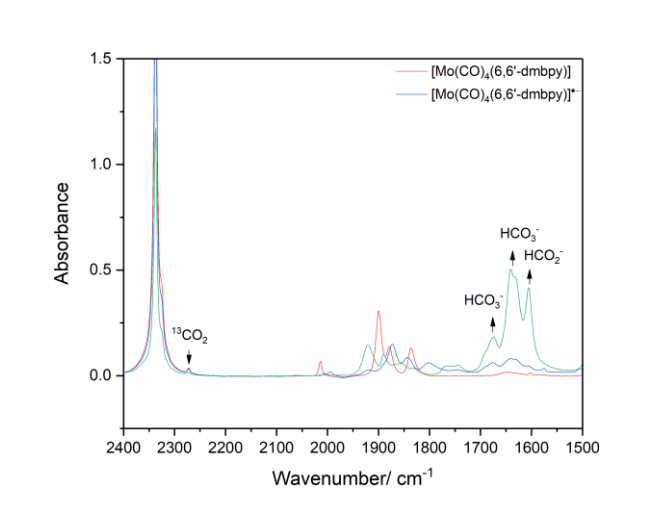

Figure S8: IR SEC monitoring of [Mo(CO)$_4$(6,6'-dmbipy)] in CO_2-saturated THF/Bu_4NPF_6 at a gold minigrid electrode. The spectral changes correspond to conversion of the parent (red) to the radical anion (blue), and the situation after the catalytic wave near R2 is passed (green).

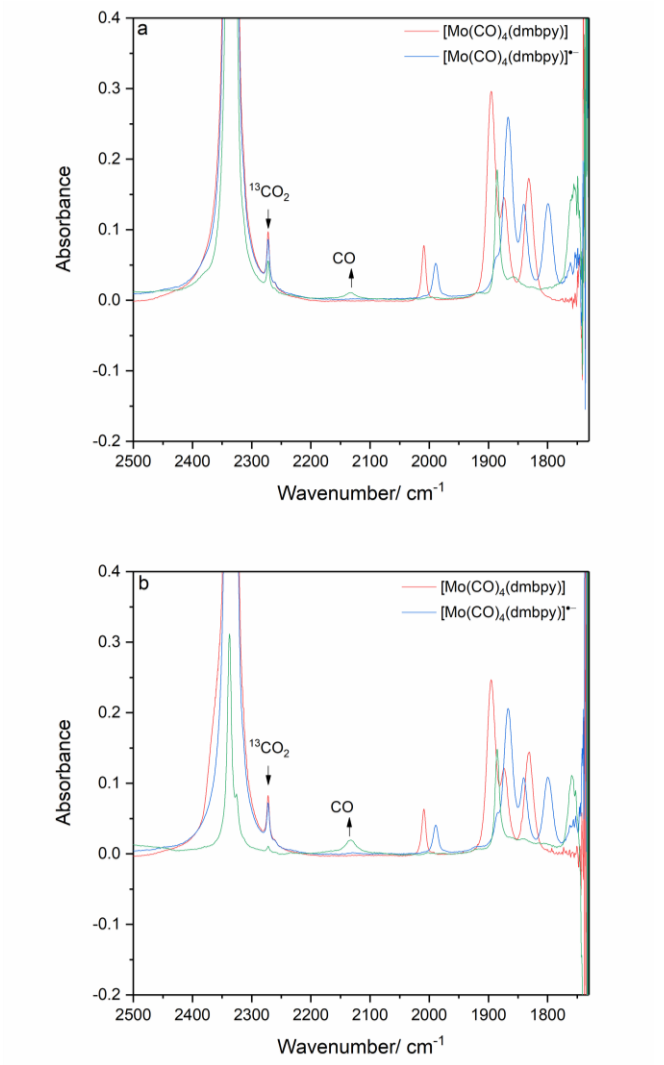

Figure S9: IR SEC monitoring of [Mo(CO)$_4$(4,4'-dmbipy)] reduction in CO_2-saturated NMP/Bu_4NPF_6 at (a) a Pt minigrid electrode and (b) an Au minigrid electrode. The spectral changes correspond to the conversion of the parent complex (red) to its radical anion (blue), and finally to the situation after the catalytic wave is passed (green).

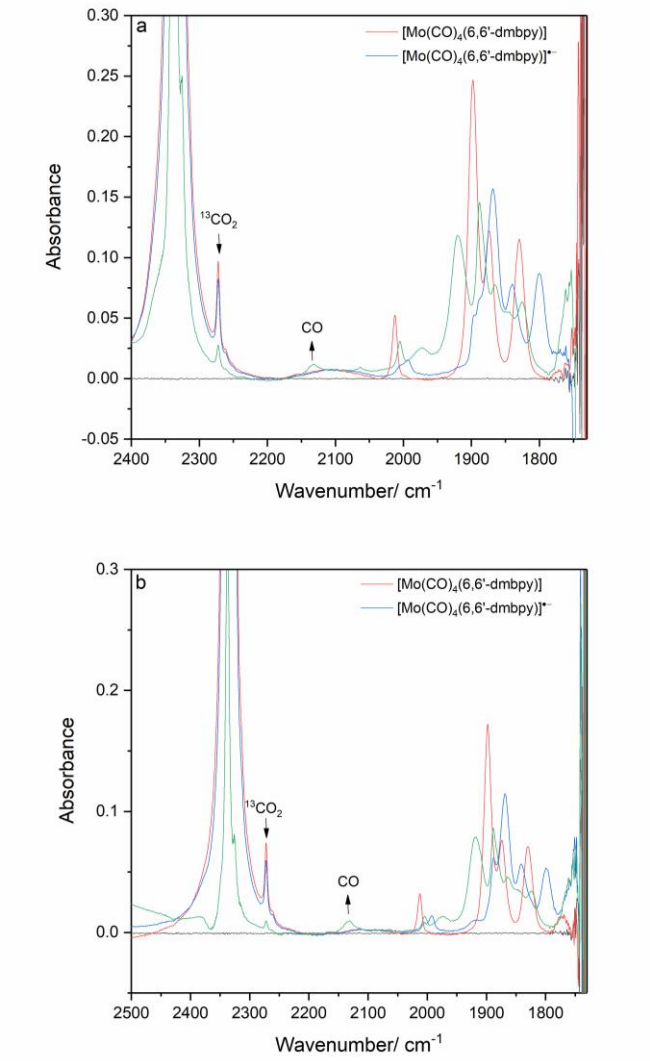

Figure S10: IR SEC monitoring of [Mo(CO)$_4$(6,6'-dmbipy)] reduction in CO_2-saturated NMP/Bu_4NPF_6 at (a) a Pt minigrid electrode, and (b) an Au minigrid electrode. The spectral changes correspond to the conversion of the parent complex (red) to its radical anion (blue), and finally to the situation after the catalytic wave is passed (green).

References

[1] M. Krejčík, M. Daněk, F. Hartl, *J. Electroanal. Chem. Interfacial Electrochem.* **1991**, *317*, 179–187.

[2] J. Tory, B. Setterfield-Price, R. A. W. Dryfe, F. Hartl, *ChemElectroChem* **2015**, *2*, 213–217.